Signature of Ericson fluctuations in helium inelastic scattering cross sections near the double ionization threshold

Junliang Xu,[1,*] Anh-Thu Le,[1] Toru Morishita,[2] and C. D. Lin[1]

[1]*Department of Physics, Kansas State University, Manhattan, Kansas 66506, USA*
[2]*Department of Applied Physics and Chemistry, University of Electro-Communications, Tokyo, 182-8585, Japan*
and PRESTO, JST, Kawaguchi, Saitama, 332-0012, Japan

We calculated the inelastic electron impact excitation cross sections of He$^+$ by electrons for a model helium atom to examine the onset of the signature of quantum chaotic scattering in this simple system. We find Ericson fluctuations (EF) in the calculated inelastic scattering cross sections only when the impact energies lie within about 0.21 eV below the double ionization threshold. We also discuss the stringent requirements and the proper methods for analyzing the inelastic scattering cross sections in order to observe EF experimentally.

I. INTRODUCTION

It is well known that the classical dynamics of the two electrons in helium is largely chaotic. Nonetheless, at low energies the quantum states of helium atom show regular progressions, and the states are accurately labeled by sets of approximate quantum numbers, including doubly excited states that have been experimentally observed so far, see Ref. [1], and references therein. Despite continuing efforts in the past two decades, it is fair to say that no clear experimental evidence of quantum chaos has emerged so far in helium. Using third-generation synchrotron radiation, photoabsorption cross sections of He have been measured up to the He$^+$($N=9$) threshold by Püttner *et al.* [2]. By analyzing the nearest-neighbor spacing (NNS) distributions of the observed resonances, it has been claimed that there is a slight evidence of quantum chaos in this energy region. Partial photoionization cross sections and angular distributions for double excitation of helium up to the He$^+$($N=13$) have been reported by Czasch *et al.* [3], but the issue of quantum chaos was not addressed.

What does it take to observe the signature of quantum chaos? One expects that the approximate quantum numbers K, T, A for each series of doubly excited states [1,4,5] cease to function as the energy of helium reaches higher N of the He$^+$(Ns) thresholds. When this occurs, the states from different series overlap strongly so that there are no good quantum numbers left, except for the possible ordering of states by the energy. Since quantum chaos is not easily uniquely defined, different criteria for measuring quantum chaos have been used. A popular one is the statistical property of the nearest-neighbor spacing distributions [6,7] which measures the fluctuations in level spacings. For quantum systems whose classical counterpart is regular, the NNS distribution generally is Poissonian. Using the Brody parameter [8], q, to measure the NNS distributions of helium, where $q=0$ gives the Poisson distributions and $q=1$ the chaotic Wigner distributions, Le *et al.* [9] examined the NNS of doubly excited states of helium and of the so-called s^2-model helium. In the simpler s^2 model the orbital angular momentum of each electron is restricted to $l=0$. For the levels with energies between He$^+$($N=14$) and He$^+$($N=19$), Le *et al.* [9] found a Brody parameter of 0.66. For s^2-model helium, they found $q=0.95$ for energy levels between He$^+$($N=25$) and He$^+$($N=30$). This study indicates that the approach to the quantum chaos limit of $q=1$ in helium is quite slow, which may serve to explain why experimental measurements of energy levels near the He$^+$($N=9$) threshold still fails to show clear signature of quantum chaos.

The characterization of quantum chaos in terms of NNS as discussed above for helium atom is not complete since the levels of doubly excited states are resonances. As the double ionization threshold is approached, the effect of the overlap and interactions among these resonances, instead of resulting in cross sections that are smooth functions of energy, actually resulting in fluctuations, termed Ericson fluctuations (EF) [10–14]. EF has been observed in nuclear physics since the 1960s [15,16], but the first experimental evidence of EF in atomic physics has been reported only recently [17] in the photoionization spectra of a Rb atom in strong crossed electric and magnetic fields. The experimental data were generated using one diode laser and one ring laser in order to achieve the high spectral resolution needed in the higher energy region.

In this paper our goal is to study the spectral properties of He in the energy regime where EF can possibly be observed. For this purpose we calculated the partial inelastic scattering cross sections between electrons and He$^+$ ions from the ground state as well as from the excited states. To reduce numerical complexity, the calculations were carried out for s^2-model helium. The partial inelastic scattering cross sections are calculated using the hyperspherical close-coupling method. We will show that resonances associated with low-lying doubly excited states are rather regular. As the total electronic energy increases local irregularities begin to appear. As the total energy further increases, the density of states becomes very large and inelastic scattering cross sections exhibit very complex structure such that identification of individual resonance becomes unattractive, if not impossible. In such a regime, it is preferable to analyze the scattering cross sections statistically, from which we will inves-

_____
*junliang@phys.ksu.edu

tigate the onset of EF in the resonances of the model helium. For this purpose, the analysis of EF has to be modified for the helium resonances. In fact, we show that EF can be clearly seen in this model helium atom only when the total electron energy is near the He$^+$(Ns) for N near and above 16, or about 0.21 eV below the double ionization threshold. Experimentally, to make sure that the fluctuations are not washed out by the instrumental resolution, we show that the resolution of the electron spectrometer would have to be better than a fraction of 1 meV.

In Sec. II we briefly summarize the theoretical model and the computational methods used in the present calculation. In Sec. III the results are analyzed, showing how the resonances, or more precisely, how the cross sections evolve with the total energy of the system. The scattering cross sections are then analyzed in terms of the autocorrelation function to examine the signature of EF or the emergence of quantum chaos. A short summary and future perspective of issues associated with EF in helium are given in the last section.

II. THEORETICAL MODEL AND COMPUTATIONAL METHODS

A. The model He atom

We are interested in the energy region very close to the double ionization threshold. We will focus first on two electrons which are coupled to total orbital and spin angular momenta $L=0$ and $S=0$. Since the number of channels increases rapidly as the total electronic energy of the system approaches the double ionization threshold, in the present calculation we will limit ourselves to the so-called s^2 model, i.e., the orbital angular momentum of each electron is limited to $l=0$ only. Doubly excited states of such a model helium have been investigated for states lying below the $N=2$ to $N=8$ thresholds of He$^+$, including their widths, by Draeger *et al.* [18]. Using this model, there is only one ^1S Rydberg series below each He$^+$(Ns) threshold. In comparison with the real helium atom, there are N Rydberg series below each He$^+$(Ns) threshold for the $L=0$ and $S=0$ symmetry.

As N increases, members of neighboring Rydberg series overlap. These levels interact strongly such that individual resonances can no longer be assigned to a given threshold. Moreover, the resonances are crowded together such that the identification of individual resonance from the spectra becomes nearly impossible, nor of general interest. We note that the s^2 model of He has also been used previously by Le *et al.* [9]. By removing the coupling of these resonances with the "background" continuum channels, the resulting energy levels were analyzed to extract their nearest-neighbor spacing distributions. The calculated NNS are then fitted to find the Brody parameter q to quantify the evolution of the levels toward the quantum chaos regime.

B. Calculation of inelastic scattering cross sections

Our calculations are based on the general hyperspherical close-coupling method [19,20]. Briefly, we replace the radial distances of the two electrons r_1 and r_2 by a hyperradius R

and a hyperangle α. The two-electron wave function is given by

$$\psi(\mathbf{r}_1, \mathbf{r}_2) = \sum_\mu F_\mu(R) \Phi_\mu(\Omega; R). \quad (1)$$

Here $\Phi_\mu(\Omega; R)$ is the adiabatic channel function which can be solved from the eigenvalue equation

$$[H_{\text{ad}}(\Omega; R) - U_\mu(R)]\Phi_\mu(\Omega; R)$$
$$= \left[\frac{\Lambda^2(\Omega)}{2R^2} + \frac{C(\Omega)}{R} - U_\mu(R) \right] \Phi_\mu(\Omega; R) = 0, \quad (2)$$

where Λ^2 is the grand angular momentum operator, C is the effective charge, U_μ is the adiabatic potential, and Ω represents the five angles $\{\alpha, \theta_1, \varphi_1, \theta_2, \varphi_2\}$ collectively [19]. And for the s^2 model, the effective charge C is obtained from the angular average of

$$C(\Omega) = -\frac{Z}{\sin \alpha} - \frac{Z}{\cos \alpha} + \frac{1}{\sqrt{1 - \sin 2\alpha \cos \theta_{12}}}, \quad (3)$$

where θ_{12} is the angle between the two electrons with respect to the nucleus. Within the s^2 model, the orbital angular momentum is taken to be zero for each electron. Thus the potential (3) is given by its spherical average and the solution of Eq. (2) becomes a simple differential equation for the hyperangle α.

In the adiabatic approach, R is treated as a slow parameter. The eigenvalues of H_{ad} give the adiabatic potential curves $U_N(R)$, with one potential curve for each N, i.e., for each channel N, and $U_N(R) \rightarrow -2/N^2 - 2/R$, as $R \rightarrow \infty$. (Atomic units are used throughout this paper unless otherwise noted.)

In the first-order approximation, one can neglect the nonadiabatic coupling among the different channels. Thus each potential curve will support one Rydberg series. Such a Rydberg series can be designated by n_N with $n = N, N+1, \ldots, \infty$. The energy for each state n_N is written using the Rydberg formula

$$E(n, N) = -\frac{2}{N^2} - \frac{1}{2[n - \sigma(n)]^2}, \quad (4)$$

where $\sigma(n)$ is the quantum defect which is nearly constant for large n. As N increases, the Rydberg series from neighboring channels begin to overlap. If there are only a few levels from the upper channel overlapping with a given Rydberg series, the spectra or the quantum defect $\sigma(n)$ will exhibit strong local variation near the position of the "intruder" level. For higher N, there are many more "intruders" and the width of each state becomes comparable or greater than the level separation. The strong interaction among them renders the identification of each level impossible. Moreover, as shown by Ericson, the resulting spectra are by no means smooth. In fact, his model predicts that the spectra show large fluctuations, and thus EF is used to characterize the global spectral behavior in this chaotic region. In this paper, we set out to show that helium spectra at energies close to the double ionization do show features similar to EF.
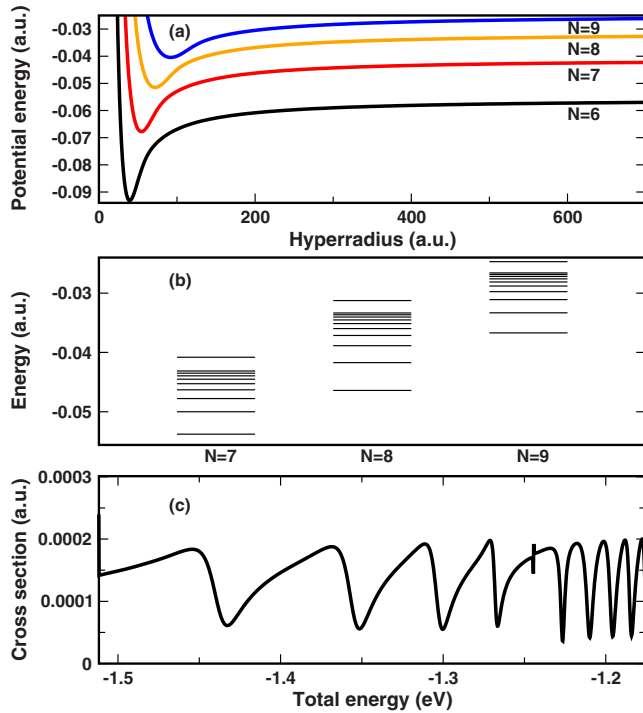
FIG. 1. (Color online) (a) Adiabatic hyperspherical potential curves for s^2-model helium for states that are associated with the He$^+(N=6)$ to He$^+(N=9)$ thresholds. (b) Energies of the bound states associated with each potential curve calculated in the single-channel approximation. (c) Partial $1s \rightarrow 5s$ inelastic scattering cross sections vs the total energy of the two electrons. The energy region covered is between the $N=6$ and $N=7$ thresholds of He$^+$.

FIG. 2. (Color online) Same as Fig. 1 but for states associated with I_{21} to I_{27} thresholds of He$^+$. In (c), inelastic scattering cross sections from $18s$ to $19s$ are calculated for the energy region between the $N=21$ and $N=22$ thresholds, vs the total energy of the two electrons.

To obtain inelastic scattering cross sections, the nonadiabatic couplings between adiabatic channels have to be included. In practical numerical calculations, the modern hyperspherical close-coupling method employs a smooth variable discretization (SVD) technique introduced by Tolstikhin *et al.* [20]. The method avoids the direct calculation and use of the nonadiabatic coupling matrix elements. First the hyperradius is divided into sectors. Within the sector, the hyperradial wave functions are expanded in terms of discrete-variable representation (DVR) basis functions in R. In the SVD, the total wave function must be smooth in the adiabatic parameter R within the sector. The total wave function is propagated from one sector to the next till a large hyperradius $R_{\max}$, where they are matched to the known asymptotic wave functions to extract the scattering matrix $S_{ij}(E)$. From the S-matrix the partial scattering cross sections are calculated. More details of the method and its applications to various three-body systems can be found in Refs. [21–26].

III. RESULTS AND DISCUSSION

A. Potential curves and energy levels

In Figs. 1 and 2 we show how the potential curves behave in the lower energy region as well as in the higher energy region. Figure 1(a) shows the four potential curves that are associated with the $N=6$, 7, 8, and 9 limits. Treating each
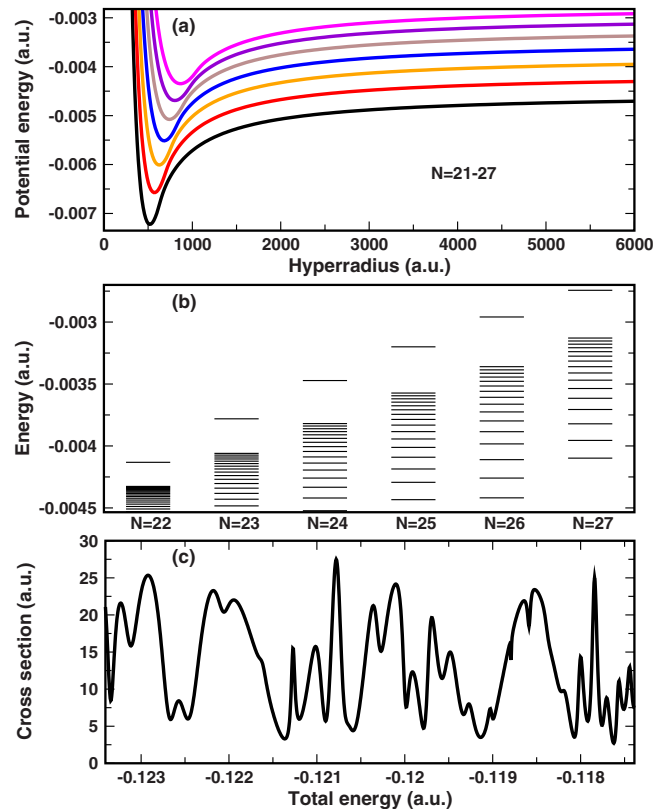
channel independently, we show in Fig. 1(b) the bound states that lie between the $N=6$ and 7 thresholds, or between I_6 and I_7. (The uppermost horizontal line along the $N=7$ series is the I_7 limit.) In this energy range, there is one Rydberg series below $N=7$ and two lowest levels from the $N=8$ threshold. The two levels from the $N=8$ threshold are the "intruders" to the $N=7$ Rydberg series. At higher energies the potential curves and energy levels overlap much more significantly. In Fig. 2(a) the potential curves from $N=21$ to 27, and in Fig. 2(b) the Rydberg levels below each threshold, are shown. For energies between I_{21} and I_{22}, the bottom of the potential well for each of the $N=23-26$ channels lies below the I_{22} limit. From Fig. 2(b), we note that the $N=22$ Rydberg series is "perturbed" by the levels from four other channels directly.

B. Inelastic scattering cross sections

The overlapping between intruder channels and the dominating channel produces irregularity in the cross sections, as shown in Figs. 1(c) and 2(c). However, the irregularities in the two spectra are different. In Fig. 1(c), the inelastic process is He$^+(1s)+e^- \rightarrow$ He$^+(5s)+e^-$ [or simply $(1s \rightarrow 5s)$] and in Fig. 2(c) it is He$^+(18s)+e^- \rightarrow$ He$^+(19s)+e^-$ $(18s \rightarrow 19s)$. Figure 1(c) shows that perturbation from $N=8$ channels leads to a local modification of an otherwise regular cross section, made up of a series of isolated resonances which could be
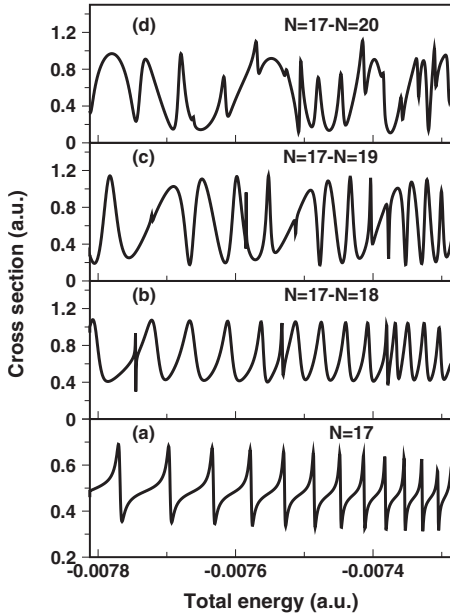
FIG. 3. Variation of inelastic scattering cross sections with the number of "intruder" channels. The cross sections shown are for the $10s \rightarrow 15s$ transitions in the energy region of I_{16} and I_{17} thresholds. (a) The uppermost channel included is $N=17$. The spectra show regular autoionizing Rydberg series. By adding the $N=18$ channel in the calculations, the intruder channel modifies the spectra locally, but also shifts the spectra (b). By adding one more channel ($N=19$) (c) and two more channels ($N=19,20$), the calculated spectra change significantly and the resulting spectra appear rather erratic, or chaotic. Note the regular sharp features as in (a) and (b) change into complicated "real" spectra as shown in (d), as the number of intruder channels increases.

labeled by the Rydberg series converging to the $N=7$ threshold. On the other hand, as the result of a larger number of "intruder" states, no individual levels can be resolved, see the display in Fig. 2(c). As the resonances are examined from the lower energies to higher energies, the cross sections evolve gradually from regular to irregular distributions.

To illustrate the strong impact of "intruders" on the cross section, we also analyzed in detail here the process $He^+(10s) + e^- \rightarrow He^+(15s) + e^-$ ($10s \rightarrow 15s$). In the energy region between I_{16} and -0.1982 eV (near I_{17}), levels from the $N=17$ series overlap with plenty of levels from the three series associated with the I_{18}, I_{19}, and I_{20} limits, respectively. We followed the change of the cross section for the $10s \rightarrow 15s$ transition by adding the "intruder" channels one by one, as shown in Fig. 3. In Fig. 3(a), only the $N=17$ channel in the four-channel overlap pattern is kept and the cross section shows typical regularity. The addition of the $N=18$ channel [see Fig. 3(b)] results in a number of local needlelike structures and also changes the profiles of the original resonances. Nevertheless, the connection of resonance features between these two calculations can still be seen. When interaction with the $N=19$ and $N=20$ channels is added sequentially [see Figs. 3(c) and 3(d)], the resulting spectra change drastically. The fluctuating features in Figs. 3(c) and 3(d) cannot be identified with individual resonances.

The calculated "chaotic" inelastic scattering cross sections in the higher energy region clearly show that the nearest-
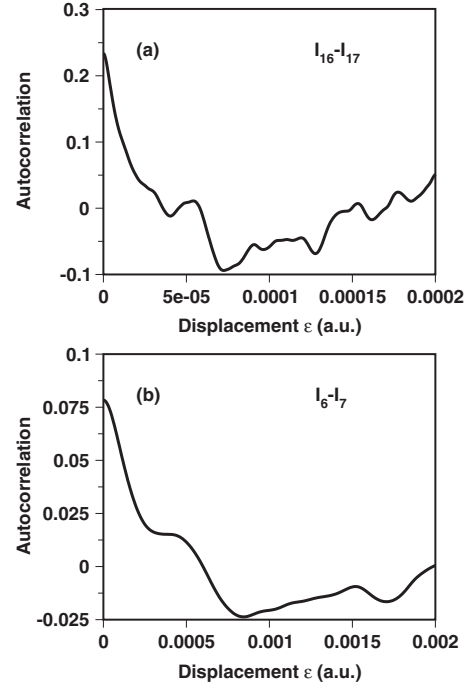

FIG. 4. Autocorrelation function extracted from cross sections on the energy scale for (a) $10s \rightarrow 15s$ excitation in the energy region between I_{16} and I_{17}. (b) Same for the $1s \rightarrow 5s$ excitation in the I_6-I_7 region. Note that the autocorrelation functions in the two energy regimes do not differ much, even though the spectra for the former is chaotic while for the latter it is quite regular.

neighbor spacing distributions cannot be used to characterize the spectral features since the resonance levels cannot be identified. The inelastic scattering cross sections should be viewed as a continuous function of the total energy where the broad or narrow structures may not be associated with the lifetimes of some particular resonances since the resonances are not identifiable. In other words, characterization of inelastic scattering cross sections in terms of resonances appears no longer a valid description of the spectra. For such complicated spectra, Ericson fluctuations provide a first-order description of the "chaotic" spectra. It is defined by the autocorrelation function [17]

$$C(\epsilon) = \langle [\sigma(E + \epsilon) - \bar{\sigma}][\sigma(E) - \bar{\sigma}] \rangle_E / \bar{\sigma}^2 \qquad (5)$$

Here $\langle \cdots \rangle_E$ means the average is integrated over the energy and $\bar{\sigma} = \langle \sigma \rangle_E$ is the mean cross section. Following the definition of Eq. (5), we show in Fig. 4(a) the calculated autocorrelation function for inelastic scattering cross sections of the $10s \rightarrow 15s$ transition for energies between I_{16} and I_{17} and in Fig. 4(b) for the $1s \rightarrow 5s$ transition for energies between I_6 and I_7. The autocorrelation functions between these two cases appear to be quite similar, despite the fact that the energy dependence of the inelastic scattering cross sections looks quite different, see Figs. 3(d) and 1(c) where the former is quite "chaotic" while the latter is quite regular. These two results show that the autocorrelation function defined in Eq. (5) is not capable of distinguishing the spectral behaviors of helium atoms in the "regular" region from the "irregular" region.
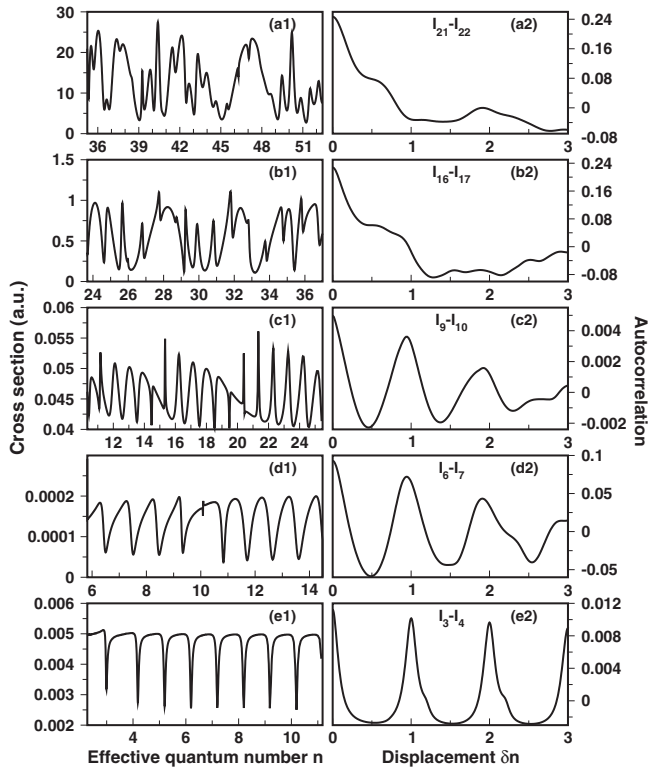
FIG. 5. Inelastic scattering cross sections expressed on the n-scale (left column) and the corresponding autocorrelation functions (right column). (a) $18s \rightarrow 19s$ excitation between I_{21} and I_{22}. (b) $10s \rightarrow 15s$ excitation between I_{16} and I_{17}. (c) $3s \rightarrow 5s$ excitation between I_9 and I_{10}. (d) $1s \rightarrow 5s$ excitation between I_6 and I_7. (e) $1s \rightarrow 2s$ excitation between I_3 and I_4.

The failure of the autocorrelation function defined by Eq. (5) to reveal regular from irregular spectra of helium resonances has been traced to the fact that the conditions used to derive Ericson fluctuations are not met in the helium spectra. In his derivation, Ericson assumed that the width of each resonance is large compared to the level separations, while the levels are fully randomly distributed. For the Rydberg levels in each series, the energies follow the $1/n^2$ progression, thus there are higher level densities at higher energies. In other words, the level distributions are not fully randomly distributed as assumed in the model of Ericson. To make the levels randomly distributed, we define energies in terms of effective quantum numbers n (as in the Rydberg formula after the energy is referred to the threshold) and calculate the "autocorrelation" function with respect to δn:

$$C(\delta n) = \langle [\sigma(n + \delta n) - \bar{\sigma}][\sigma(n) - \bar{\sigma}] \rangle_n / \bar{\sigma}^2. \quad (6)$$

In Fig. 5 the main results of this work are presented. The inelastic scattering cross sections displayed using the n scale are shown for scattering energies between I_3 and I_4, I_6 and I_7, I_9 and I_{10}, I_{16} and I_{17}, and I_{21} and I_{22}, for $1s \rightarrow 2s$, $1s \rightarrow 5s$, $3s \rightarrow 5s$, $10s \rightarrow 15s$, and $18s \rightarrow 19s$ transitions, respectively. In the low-energy region, the cross section consists of a series of equal-spaced isolated resonances, and the autocorrelation function shows perfect periodicity [see Fig. 5(e)]. Moving to the higher energies, this periodicity is gradually

destroyed, and the autocorrelation function on the n scale drops from the maximum at $\delta n = 0$ following a function that is nearly Lorentzian, as described in the theory of Ericson fluctuations.

These results are summarized here: At low energies, the correlation is long ranged, and the two isolated resonances far from each other are still closely correlated; at high energies, the correlation in the cross section is short-ranged, and the degree of correlation between two points in the cross section curve decreases quickly as the distance increases. Autocorrelation in n scale provides a clear tool for specifying how "chaos" emerges in the language of Ericson fluctuations.

C. Evidence of Ericson fluctuations in the resonant energy spectra of helium

The autocorrelation functions $C(\delta n)$ for resonances with energy between I_{16} and I_{17} and between I_{21} and I_{22}, shown in Figs. 5(a2) and 5(b2), respectively, are the main results of this work. They show similarity to the Lorentzian shape for small δn as predicted by Ericson's model. However, the autocorrelation function actually shows significant deviations from Lorentzian for larger δn. In fact, the $C(\delta n)$ we obtained from the model helium atom is actually much closer to the equivalent $C(\epsilon)$ found by Stania and Walther [17] (see their Fig. 3), from analyzing the photoabsorption spectra of ^{87}Rb in strong crossed magnetic and electric fields in the energy regime beyond the ionization threshold. Both our $C(\delta n)$ and their $C(\epsilon)$ show kinks away from the smooth Lorentzian dependence and become negative for large δn or ϵ. In fact, the observed photoabsorption spectra and the $C(\epsilon)$ of ^{87}Rb have been reproduced from *ab initio* numerical calculations by Madronero and Buchleitner [27]. A similar behavior of $C(\epsilon)$ has also been found in the theoretical study of transmission through microwave cavities as well as through many toy-model systems [28].

From the analysis of the helium spectra, we found that the parameter characterizing the general behavior of Ericson fluctuations is not necessarily given by ϵ. For helium or any atomic systems, the Rydberg levels tend to cluster toward each threshold. By using the n scale for the energy in helium, the distribution of resonances is treated on equal footing in that n can be considered to be a genuine random number. This condition lies at the heart of the derivation of EF. Using the n scale for energy, we claim that the autocorrelation function shown in Figs. 5(a2) and 5(b2) demonstrate EF in the helium spectra in the indicated energy region.

D. Practical issues associated with observing Ericson fluctuations in helium

The discussion so far on the scattering cross sections assumes that the electron energy can be measured with "infinite" resolution. In actual experiments, one has to deal with energy resolution of the spectrometer. We have shown that clear indication of EF occurs when the total energy is near about I_{16} from Fig. 5. That is, about 0.21 eV below the double ionization threshold. By introducing experimental resolutions, sharp structures in the cross sections will be
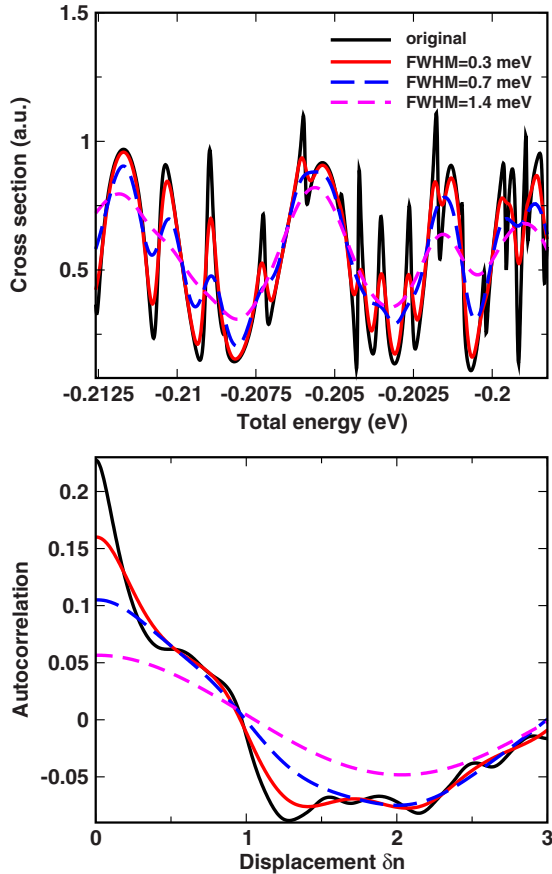
FIG. 6. (Color online) Illustration of how the "chaos" in the electron spectra between I_{16} and I_{17} and the corresponding autocorrelation functions are washed out by the energy resolution of the electron spectrometer. Gaussian functions with FWHMs of 0.3, 0.7, 1.4 meV are used to convolute the spectra, respectively.

smoothed out. This is illustrated in Fig. 6 by convoluting the calculated cross section with a Gaussian profile with full widths at half maximum (FWHMs) of 0.3, 0.7, and 1.4 meV, respectively. Such resolutions are very difficult to achieve today except for lasers. In the convoluted cross sections, the sharp features are removed, as seen in Fig. 6(a), and the corresponding autocorrelation function in the n scale, while still preserving the Lorentzian shape near $\delta n = 0$, the slope and the contrast are significantly reduced as the resolution of the spectrometer is reduced. The most recent experiment on He spectrum near the double ionization limit was reported by Czasch *et al.* [3] where cross sections near the I_{13} and below were examined. The resolution of the electrons reported in that paper was about 3.9 meV. While they did not make an effort to search for Ericson fluctuations in their paper, our analysis given here would show that the evidence, if ever exists there, would be very difficult to unravel, unless the spectra are measured with much higher resolution (not possible) and are analyzed systematically following the outline shown in Figs. 5 and 6. EF cannot be visualized directly by looking at the "raw" data alone.

IV. SUMMARY AND PERSPECTIVE

In this paper we search for evidence of Ericson fluctuations in the inelastic scattering cross sections of a model

helium atom in the energy region very close to the double ionization threshold. By limiting ourselves to the s^2 model where the angular momentum of each electron is limited to $l = 0$, we are able to calculate the inelastic scattering cross sections in the energy region very close to the double ionization threshold. In this model the energy scale is similar to the real helium atom, but the dimension of the system is reduced from 6 to 2 such that the inelastic scattering cross sections can be calculated accurately using the well-established hyperspherical close-coupling method. As the total energy is increased, inelastic scattering cross sections evolve from the familiar well-separated isolated resonances or locally perturbed resonances, to the high energy region where individual resonances are no longer identifiable. We found that for energies above the $N = 16$ or 17 limit of He$^+$ (or about 0.21 eV below the double ionization limit), the inelastic scattering cross sections look very irregular. Such spectra are best analyzed statistically. By calculating the autocorrelation function, we found that indeed it has the Lorentzian shape as predicted by Ericson, thus revealing signature of quantum chaos in these energy regimes. However, we also showed that EF can be seen only if the energy is expressed in the n scale, where n is the principal quantum number when the energy is measured from the given N threshold. We also showed that the autocorrelation function for He deviates from the prediction of Ericson for larger δn, but it is very similar to the autocorrelation function derived from the absorption spectra of ^{87}Rb atoms in strong crossed electric and magnetic fields. Even though the s^2 model was used in the calculation, the general conclusion should be similar for the true 3D helium atom since the energy separations and the density of the resonances are about the same. Comparison of the two models for the nearest-neighbor spacing distributions has been carried out in Le *et al.* [9].

Experimentally, the signature of quantum chaos in helium spectra has been studied by Püttner *et al.* [2], by analyzing the nearest-neighbor spacing distributions for resonances below I_9. They claimed seeing evidence of the onset of quantum chaos by analyzing the photoabsorption spectra for energies below I_9. Theoretical calculations by Le *et al.* [9] in the same spectral region failed to draw the same conclusion, where in the latter the "signature" of quantum chaos is measured in terms of the Brody parameter. Since the work of Püttner *et al.*, Czasch *et al.* [3] recently reported the partial photoionization cross sections of He for energies up to the $N = 13$ threshold. The achievable photon energy resolution is about 2.0 to 3.9 meV. The observed complicated spectra were analyzed by comparing with the spectra calculated from the R-matrix method [29] showing good agreement. However, resolutions of a few meV, based on the results from Fig. 6, are likely to wash out any sharp features in the spectra and thus distort the derived autocorrelation function.

Based on the present analysis we conclude that it is nearly impossible to find irrefutable evidence of Ericson fluctuations in the spectra of helium using the currently available third-generation synchrotron radiation. To study the spectra with the resolutions indicated in Fig. 6 or better, probably one has to wait till the next-generation light sources based on free-electron lasers becomes available. Since sharp features in the spectra imply long time behavior, alternatively, in the

future, one may want to examine the time-dependent behavior of the electron wave packet where their energy spectra exhibit EF [30]. From the quantum-classical correspondence, the quantum dynamics is expected to follow the classical dynamics quasideterministically. The random wave interference is only established after a finite time, the so-called Ehrenfest time [31]. Recent rapid progress in ultrafast light sources may make such time-dependent measurements feasible in the foreseeable future. Already the Auger lifetime has been directly measured in the time domain [32]. The time evolution of an isolated autoionizing resonance in the streaking laser field [33,34] and the time-resolved correlated motion of the two electrons of He using attosecond light pulses [35] has also been studied theoretically. It will be of extreme interest to begin investigating the time evolution of a wave packet constructed from states in the spectral region where the inelastic scattering cross sections exhibit Ericson fluctuations. Measurements of such wave packets would allow laboratory investigations of how the dynamical description of a quantum system merges into the classical limit and in what way the quantum interference remains.

ACKNOWLEDGMENTS

[1] C. D. Lin, *Advances in Atomic and Molecular Physics* (Academic, New York, 1986), Vol. 22, pp. 77–142.

[2] R. Püttner, B. Grémaud, D. Delande, M. Domke, M. Martins, A. S. Schlachter, and G. Kaindl, Phys. Rev. Lett. **86**, 3747 (2001).

[3] A. Czasch *et al.*, Phys. Rev. Lett. **95**, 243003 (2005).

[4] C. D. Lin, Phys. Rev. A **29**, 1019 (1984).

[5] D. R. Herrick and M. E. Kellman, Phys. Rev. A **21**, 418 (1980).

[6] O. Bohigas, M. J. Giannoni, and C. Schmit, Phys. Rev. Lett. **52**, 1 (1984).

[7] E. P. Wigner, in *Proceedings of the Fourth Canadian Mathematical Congress*, edited by M. S. MacPhail (University of Toronto Press, Toronto, 1959), p. 174.

[8] T. A. Brody *et al.*, Rev. Mod. Phys. **53**, 385 (1981).

[9] A. T. Le, T. Morishita, X. M. Tong, and C. D. Lin, Phys. Rev. A **72**, 032511 (2005).

[10] T. Ericson, Phys. Rev. Lett. **5**, 430 (1960).

[11] T. Ericson, Ann. Phys. (N.Y.) **23**, 390 (1963), and references therein.

[12] R. Blümel and W. P. Reinhardt, *Chaos in Atomic Physics* (Cambridge University Press, Cambridge, England, 1997), pp. 234–239.

[13] S. Y. Kun, Phys. Rev. A **65**, 034701 (2002)

[14] R. Blümel and U. Smilansky, Phys. Rev. Lett. **60**, 477 (1988).

[15] P. von Brentano, J. Ernst, O. Häusser, T. Mayer-Kuckuk, A. Richter, and W. Von Witsch, Phys. Lett. **9**, 48 (1964).

[16] T. Ericson and T. Mayer-Kuckuk, Annu. Rev. Nucl. Sci. **16**, 183 (1966) and references therein.

[17] G. Stania and H. Walther, Phys. Rev. Lett. **95**, 194101 (2005).

[18] M. Draeger, G. Handke, W. Ihra, and H. Friedrich, Phys. Rev. A **50**, 3793 (1994).

[19] C. D. Lin, Phys. Rep. **257**, 1 (1995).

[20] O. I. Tolstikhin, S. Watanabe, and M. Matsuzawa, J. Phys. B **29**, L389 (1996).

[21] C. N. Liu, A. T. Le, T. Morishita, B. D. Esry, and C. D. Lin, Phys. Rev. A **67**, 052705 (2003).

[22] D. Kato and S. Watanabe, Phys. Rev. A **56**, 3687 (1997).

[23] O. I. Tolstikhin and H. Nakamura, J. Chem. Phys. **108**, 8899 (1998).

[24] T. Morishita, K. Hino, T. Edamura, D. Kato, S. Watanabe, and M. Matsuzawa, J. Phys. B **34**, L475 (2001).

[25] A. T. Le, C. N. Liu, and C. D. Lin, Phys. Rev. A **68**, 012705 (2003).

[26] A. T. Le, M. Hesse, T. G. Lee, and C. D. Lin, J. Phys. B **36**, 3281 (2003).

[27] J. Madronero and A. Buchleitner, Phys. Rev. Lett. **95**, 263601 (2005).

[28] E. N. Bulgakov, I. Rotter, and A. F. Sadreev, Phys. Rev. B **76**, 214302 (2007).

[29] T. Schneider, C. N. Liu, and J. M. Rost, Phys. Rev. A **65**, 042715 (2002).

[30] T. Gorin, D. F. Martinez, and H. Schomerus, Phys. Rev. E **75**, 016217 (2007).

[31] I. L. Aleiner and A. I. Larkin, Phys. Rev. B **54**, 14423 (1996).

[32] M. Drescher *et al.*, Nature (London) **419**, 803 (2002).

[33] Z. X. Zhao and C. D. Lin, Phys. Rev. A **71**, 060702(R) (2005).

[34] M. Wickenhauser and J. Burgdörfer, Laser Phys. **14**, 492 (2004).

[35] T. Morishita, S. Watanabe, and C. D. Lin, Phys. Rev. Lett. **98**, 083003 (2007).